Web: http://ascelibrary.org/doi/10.1061/%28ASCE%29ST.1943-541X.0001831

Cite: Silva, L. C., Lourenço, P. B., and Milani, G. (2017). "Nonlinear Discrete Homogenized Model for Out-of-Plane Loaded Masonry Walls." *Journal of Structural Engineering*, 143(9).

Nonlinear discrete homogenized model for masonry walls out-of-plane loaded

Luís C. Silva[(1)], Paulo B. Lourenço[(2)], Gabriele Milani[(3)]

[1] PhD candidate, Dept. of Civil Engineering, ISISE, University of Minho, Azurém, 4800-058 Guimarães, Portugal. E-mail: luisilva.civil@gmail.com

[2] Full Professor, Dept. of Civil Engineering, ISISE, University of Minho, Azurém, 4800-058 Guimarães, Portugal. E-mail: pbl@civil.uminho.pt

[3] Associate Professor, Department of Architecture, Built environment and Construction engineering (A.B.C.), Technical University in Milan, Piazza Leonardo da Vinci 32, 20133 Milan, Italy. E-mail: gabriele.milani@polimi.it

Keywords: masonry, out-of-plane, homogenization, nonlinear, DEM

Abstract

A simple and reliable homogenization approach coupled with rigid elements and homogenized interfaces for the analysis of out-of-plane loaded masonry panels is presented.

The homogenization approach proposed is a coarse FE discretization where bricks are meshed with a few elastic constant stress triangular elements and joints reduced to interfaces with elasto-plastic softening behavior with friction, tension cutoff and a cap in compression. Flexural behavior is deduced from membrane homogenized stress-strain relationships through thickness integration (Kirchhoff-Love plate hypothesis). The procedure is robust and allows obtaining homogenized bending moment/torque curvature relationships (also in presence of membrane pre-compression) to be used at a structural level within a Rigid Body and Spring Mass model (RBSM) implemented in the commercial code ABAQUS. The model relies in rigid quadrilateral elements

interconnected by homogenized bending/torque nonlinear springs. The possibility of extending the procedure to the FE-package ABAQUS, with standard built-in solution procedures, allows for a robust reproduction of masonry out-of-plane behavior beyond the peak load, in presence of global softening.

The procedure is tested on a set of windowed and full masonry panels in two-way bending. Excellent agreement is found both with experimental data and previously presented numerical approaches.

Introduction

Out-of-plane failure of masonry occurs at very low levels of the horizontal actions and there are three main features to deal with in a numerical model devoted to the analysis of masonry in bending: (1) the role of vertical membrane pre-compression, (2) masonry orthotropic behavior due to the arrangement of the units, and (3) possible failure due to out-of-plane shear in case of thick walls. A vertical membrane pre-compression, typically due to masonry self-weight and gravity loads in general, plays a fundamental role in the increase in the ductility and the out-of-plane strength, as extensively shown by Milani and Tralli (2011).

Masonry orthotropy is evident for walls exhibiting a regular texture. Masonry units staggering is responsible for a horizontal bending (i.e. with rotation along a vertical axis) stiffer and more resistant than the vertical one (i.e. with rotation along a horizontal axis), as the bed joint contributes in torque to increase stiffness and strength. Orthotropy tends to become more evident with the progressive degradation of the material. The different topology of the continuous horizontal joints with respect to the vertical ones, interrupted by the blocks, implies that tangential stresses acting on bed joints tend to play a significant role in the horizontal bending increase, while they are not relevant in vertical bending. Micro-modelling, relying into the distinct discretization of units and mortar (usually reduced to interface to speed up computations) is certainly capable of well reproducing out-of-plane orthotropy, see for instance Macorini & Izzuddin (2011) and Macorini & Izzuddin (2013), but such procedure is characterized by long processing times and a large number of degrees of freedom, sometimes requiring parallelization.

Considering the difficulties, it can be affirmed that at present a macro-scale computational approach is still needed. Macro-modelling (Dhanasekar et al. 1985; Lourenço 1997, 2000; Pelà et al. 2013) allows studying large scale structures without the drawbacks exhibited by micro-modelling, because the heterogeneous assemblage of mortar and bricks is substituted at a structural scale with a fictitious homogeneous anisotropic material. The calibration of the model is however cumbersome, as a consequence of the high level of sophistication, usually needing several inelastic parameters to set, requiring expensive experimental campaigns and data (Lourenço et al. 1998).

It is noted that it is not straightforward to account for tangential stresses acting along the out-of-plane direction. This would require to deal with 3D models at the meso-scale, as well as to adopt 3D strength domains and 3D inelastic strain evolution laws for mortar joints reduced to interfaces. For running bond and generally for single or two-wythes walls (e.g. English or Flemish bond) with slenderness greater than 8-10, it has been shown by different authors (Casolo and Milani 2010; Cecchi et al. 2007; Cecchi and Milani 2008; Milani et al. 2006) that the assumption of the thin plate Kirchhoff–Love hypothesis is adequate and that out-of-plane sliding can occur on limited portions of the walls, mainly near corners or under concentrated loads. Therefore, at the macro-scale, damage mechanisms can be reasonably described assuming a thin plate hypothesis, i.e. where inelastic dissipation is mainly due to the combination of vertical, horizontal bending and torsion. Considering the aforementioned key issues characterizing masonry subjected to out-of-plane loading, a simple two-step model is used here to analyze efficiently masonry panels in bending.

In such a framework, homogenization (see e.g Luciano and Sacco 1997; de Buhan and de Felice 1997; Mistler et al. 2007; Milani 2011) is probably the most efficient compromise between micro- and macro-modelling, because it allows in principle to perform nonlinear analyses of engineering interest without a distinct representation of bricks and mortar, but still taking into account their mechanical properties and masonry texture at a cell level.

Homogenization (or related simplified approaches) is essentially an averaging procedure performed at a meso-scale on a representative element of volume (RVE), which generates the masonry pattern by repetition. On the RVE, a Boundary Value Problem BVP is formulated, allowing an estimation of the expected average masonry behavior to be used at structural level. The resultant material obtained is orthotropic, with softening in both tension and compression. A straightforward approach to solve BVPs at the meso-scale is based on Finite Elements (FEs) (Massart et al. 2007; Mercatoris and Massart 2011), where bricks and mortar are either elasto-plastic with softening or damaging materials. It is also known as a multilevel finite element method (FE^2), which essentially is a twofold discretization, the first for the unit cell and the second at structural level. However, FE^2 appears still rather demanding, because a new BVP has to be solved numerically for each load step, in each Gauss integration point.

In order to circumvent such a limitation, a two-step homogenization procedure is hereafter proposed. In the first step, masonry is substituted with a macroscopic equivalent material through a simplified homogenization model in which the unit cell is subdivided into several layers along the thickness. The choice of concentrating non-linearity on the interfaces appears particularly suitable because: (1) it allows limiting the computational effort required to perform full scale analyses to a great extent, and; (2) it seems in agreement with experimental evidence, clearly showing a damage propagation zigzagging along joints. Considering a single masonry layer, the RVE is discretized through triangular elastic plane stress elements (blocks) and nonlinear interfaces (mortar joints). The procedure is robust and allows obtaining homogenized bending moment/torque curvature relationships (also in presence of membrane pre-compression) to be used at a structural level.

In the second step, entire masonry walls are analyzed in the nonlinear range by means of a Rigid Body and Spring Mass model (RBSM) implemented in the commercial code Abaqus (2006). The RBSM model relies into a discretization with rigid quadrilateral elements interconnected by homogenized bending/torque nonlinear springs. It is stressed that the RBSM model is not available in ABAQUS, but it can be easily implemented utilizing the FEs gallery available in any commercial code. Standard arc-length routines already built in Abaqus (2006) allow for a robust reproduction of out-of-plane masonry behavior beyond the peak load, in presence of global softening. The latter addresses the main drawback of previous work (Milani and Tralli 2011) whereby an energy-based formulation at a structural scale was used, through a quadratic-programming approach, which assumed linear piecewise discontinuous functions for the homogenized bending curves to be able to account for material softening. The main novelty of the present study is that it allows using homogenized curves, derived from the foregoing scale, without the need of further simplifications to reproduce softening.

Two sets of structural comparisons are discussed here to show the capabilities of the procedure proposed, the first on solid walls and the second on windowed panels in two-way bending, for which global pressure-displacement and crack patterns are available from both experimental data and previously presented numerical models.

Out-of-plane homogenized model

A multi-scale approach is presented for the out-of-plane study of running-bond masonry panels, as schematically described in Fig. 1a. The figure briefly shows the proposed flow-work and the two-step strategy that firstly relies in a homogenization procedure at a meso-scale. This theory focuses on the periodicity feature of a given media and it is therefore a proper strategy for masonry (Pegon and Anthoine 1997). Again, the concept is based on the mechanical characterization of a representative volume element (hereafter, RVE) by solving a boundary value problem. Then, the study of the structure is accomplished through the assemblage of these RVE units. The strategy allows defining the mechanical properties of each material at the unit cell only, and obtaining the damage stress and strain response by introducing considerations at the component level.

Several studies showed the clear advantages of this process. It allows a good trade-off between consumed time and results accuracy and enables the study of real scale buildings, see Milani and Tralli (2011), Milani and Venturini (2011), Casolo and Milani (2013), Akhaveissy and Milani (2013) and Milani et al. (2007). The present out-of-plane homogenization model is based on the initial in-plane identification of an elementary cell. The main features of the in-plane homogenized model will be explained in what follows, for further information the reader is recommended to Milani and Tralli (2011).

The RVE Y (or elementary cell) contains all the information necessary for describing the macroscopic behavior of an entire wall. In brief, homogenization consists in introducing averaged quantities for macroscopic strain and stress tensors ($\boldsymbol{E}$ and $\boldsymbol{\Sigma}$, respectively). This is the main concept of the homogenization process and implies that the macroscopic stress $\boldsymbol{\Sigma}$ and strain $\boldsymbol{E}$ tensors are calculated as given by Eq. (1):

$$\boldsymbol{E} = \langle \boldsymbol{\varepsilon} \rangle = \frac{1}{V}\int_Y \boldsymbol{\varepsilon}(\boldsymbol{u})\, dY \;\; ; \;\; \boldsymbol{\Sigma} = \langle \boldsymbol{\sigma} \rangle = \frac{1}{V}\int_Y \boldsymbol{\sigma}\, dY \qquad (1)$$

where <*> is the average operator, $\boldsymbol{\varepsilon}$ is the local strain value, which is directly dependent on the displacements field $\boldsymbol{u}$, $\boldsymbol{\sigma}$ is the local stress value and V is the volume of the elementary cell.

The homogenization procedure allows to describe the macroscopic level through the meso-scale by means of an upward scheme. All the mechanical quantities are considered as additive functions and periodicity conditions are imposed on the stress field $\boldsymbol{\sigma}$ (see Eq.(2) and the displacement field u (see Eq.(3)) (Anthoine 1995), so that:

$$\boldsymbol{\sigma} \text{ periodic on } \partial \mathrm{Y} \text{ and } \boldsymbol{\sigma}\mathbf{n} \text{ antiperiodic on } \partial \mathrm{Y}_1 \quad (2)$$

$$\mathbf{u} = \mathbf{E}\mathrm{y} + \mathbf{u}^{\mathbf{per}} \text{ periodic on } \partial \mathrm{Y}_1 \quad (3)$$

where $\boldsymbol{u}^{per}$ stands for a periodic displacement field. It may be noted that the periodic displacement fluctuation $\boldsymbol{u}^{per}$ in Eq.(3) enforces the boundary segments of the RVE to have the same deformed configuration, see Fig. 1b.

In the present model, the RVE is constituted by joints reduced to interfaces with zero thickness and elastic bricks. Bricks are discretized by means of a coarse mesh constituted by plane-stress triangles, Fig. 1b. Likewise, brick-brick interfaces are elastic and therefore they do not contribute on the inelastic deformation of the unit cell. The utilization of brick-brick interfaces may be useful when dealing with low strength units. Here, it is assumed that all the nonlinearity in the RVE is concentrated exclusively on joint interfaces. The elastic domain of joints is bounded by a composite yield surface that includes tension, shear and compression failure with softening. A multi-surface plasticity model is adopted, with softening, both in tension and compression (see Fig. 1b). The joints failure is ruled by a classical Mohr-Coulomb type strength criterion, with a tension cut-off and a linear compression cap. The parameters f_t and f_c are, respectively, the tensile and compressive strength of the mortar, c is the cohesion, Φ is the friction angle, and Ψ is the angle which defines the linear compression cap. For the tension mode, exponential softening on the tensile strength is assumed with an associated flow-rule. The yield function reads:

$$f_1(\boldsymbol{\sigma}, \kappa_1) = \boldsymbol{\sigma} - f_0 e^{\frac{f_{t0}}{G_f}\kappa_1} \tag{4}$$

where f_{t0} is the initial joint tensile strength, G_f^I is the mode-I fracture energy and κ_1 is a scalar that controls the amount of softening. For the shear mode, a Mohr-Coulomb yield function with a non-associated flow rule is considered:

$$f_2(\boldsymbol{\sigma}, \kappa_2) = |\tau| + \boldsymbol{\sigma} \times \left(\tan(\phi_0) + \frac{(\tan(\phi_t) - \tan(\phi_0)(c_0 - c)}{c_0}\right) - c_0 e^{\frac{c_0}{G_f^{II}}\kappa_2} \tag{5}$$

where c_0 is the initial cohesion, $\tan(\phi_0)$ the initial friction angle, $\tan(\phi_t)$ the residual friction angle and $G_f^{II}$is the mode-II fracture energy. For the compression mode, an associated elastic-perfectly plastic behavior is assumed, with a yield function described as follows:

$$f_3(\boldsymbol{\sigma}) = |\tau| + (\boldsymbol{\sigma} + f_c)\tan(\Psi) \tag{6}$$

where f_c is the uniaxial compressive strength and Ψ is the angle that defined the linear compression cap. The properties adopted for the present study are gathered on Table 1. The latter information is related with the experimental data used for the validation step at a structural level of the proposed discrete model.

The response of the RVE under out-of-plane actions is obtained subdividing the thickness into several n layers (40 layers are assumed). A displacement driven approach is adopted, meaning that macroscopic curvature increments $\Delta\chi_{11}$, $\Delta\chi_{22}$, $\Delta\chi_{12}$ are applied through suitable periodic boundary displacement increments. Thus, each layer undergoes only in-plane displacements and may be modelled through plane stress FEs. Each increment defines the number of discrete data points of σ-ε and M-θ curves.

Thus, a bending moment-curvature relationship is obtained for each interface angle; through the obtained RVE macroscopic mode-I stresses. The latter failure mode assumption is valid once masonry presents in general low compressive stresses at failure. Being a low-tensile strength material, the cross-section failure is ruled by tensile cracking and a linearized behavior in compression is considered, with stiffness degradation present only in tension. Towards the derivation of the M-θ curve for each interface, the cross-section equilibrium is iteratively calculated accounting for potential pre-compression states. The bending moment capacity M of the cross section is calculated by the summation of each n_i layer contribution by means of the following equation:

$$M = \sum_{i=1}^{n} \sigma_i \bar{d}_L \, dA_i \tag{7}$$

where σ_i is the mean stress at each layer, $\overline{d_L}$ is the distance between the centroid of each layer and the neutral axis and dA_i is the area of each layer. The resultant moment M can also be simply written as the integral of stress multiplied by its distance from the middle section through the wall thickness:

$$M = \langle \boldsymbol{\sigma} y_3 \rangle = \frac{1}{A} \int_Y \boldsymbol{\sigma} y_3 \, dY \tag{8}$$

In this way, homogenized curves are approximated to define the nonlinear flexural behavior of the interfaces. The on-thickness integration hypothesis allows evaluating moment-curvature diagrams for solid brick masonries, but can be easily adapted to hollow bricks assuming different mechanical properties for, e.g. internal and external layers. The latter procedure is represented in Fig. 2 for a horizontal interface, hereafter labelled with orientation $\theta = 90$ degrees, i.e. vertical bending. A similar strategy is performed to derive the torsion moment curve. Interface orientations are guided by the mesh representation of the discrete model at a structural scale. So, the implementation in a finite element package at a macro-scale allows to represent and study three-dimensional structures under out-of-plane actions.

Structural discrete model

On a macro-scale level, the out-of-plane analysis of the masonry walls is performed through a novel discrete element mechanical system. The latter has support and background in the works by Kawai (1977) and employs the information of the homogenized curves at a structural scale. Simply, the discrete model is described as the assemblage of quadrilateral rigid plates inter-connected on interface vertices by a set of rigid beams and deformable trusses. The system of deformable trusses carries the material information required for interfaces. A decoupled characterization of flexural and torsional actions is adopted. In the mid-span of each interface a spherical hinge is positioned. The aim is to allow the rotation for torsional movements as well as to guarantee the deformed shape compatibility between adjoining elements. For a clear understanding of the model, the discrete system is represented in Fig. 3.

Such discrete element approach is implemented into a commercial finite element software, namely Abaqus (2006). The inherent advantages are mainly two. Firstly, the robustness of the software to solve nonlinear static problems in presence of material softening is obtained by means of an established arc-length procedure (Memon and Su 2004). Secondly, this allow a great potential to extend the model to structural applications in any finite element software and the possibility to be used by professionals and researchers.

Material Properties: from meso- to macro-scale

The masonry behavior when out-of-plane loaded is highly dependent on its anisotropy at failure (Gilbert et al. 2006; Milani and Lourenço 2010). Experimental information conducted on masonry walls in two-way bending shows that failure occurs for a relatively ductile behavior and forming a well-defined path, see Chong et al. (1994) and Southcombe et al. (1995).

Aiming at developing the required material information at a macro-scale, an identification of the desired mesh dimensions and geometrical characteristics of the walls may be performed. Bearing in mind that quadrilateral elements are assumed, two different angles are considered for the interfaces: 0 and 90 degrees. The behavior of the interfaces is obviously orthotropic with softening, because it derives from the aforementioned homogenization strategy. In this way, the homogenized bending moment-curvature and torsional moment-curvature curves of the interfaces is depicted in Fig. 4.

The procedure described in what follows is required to convert the latter information in valid input data for the FE package used at a structural scale. To accomplish this goal, obtaining stress and strain curves for each angle of the interface and for each bending moment direction is mandatory. Thus, the approach offers the possibility to reproduce the material orthotropy by defining different input stress-strain relationships according to the trusses' plane. The conversion between bending and torsion moment and stress values is achieved by Eq.(9) and (10):

$$\sigma_{Axial\ truss} = \frac{M l_{influence}}{A_{Axial} t} \quad (9)$$

$$\sigma_{Torque\ truss} = \frac{M l_{influence}}{A_{Torque} H} \quad (10)$$

Here, M is the bending moment, $l_{influence}$ is the influence length of each truss, t is the thickness of the wall, H the length of each quadrilateral panel, A_{Axial} is the axial truss area given by 0.25×t×H and A_{Torque} is the torque truss area given by 0.5×e×H, where e (value of 10 mm) is the gap between the rigid plates, which ideally should be zero but in practice is assumed small enough to be able to place trusses between elements.

At last, the stress homogenized input curves may be properly calibrated. An elastic calibration for the stress curves is conducted. Briefly, by assuring the energy equivalence between the discrete mechanism and a homogeneous (for the masonry data, see Table 1) continuous shell element. The latter is guaranteed separately for both flexural and torsional movements and so, a decoupled behavior is derived. For the sake of conciseness, the theoretical demonstration is not shown, but it can be easily derived that the Young's moduli of axial ($E_{flexural}$) and torque trusses (E_{torque}) are:

$$E_{flexural} = \frac{E_{masonry}e}{12l_{influence}+6e}\frac{E_{masonry}}{(1-v^2)}\, and\ E_{torque} = \frac{t^4}{3(2l_{influence}+e)H^2e}\frac{E_{masonry}}{(1+v)} \quad (11)$$

It is important to state that the present study focuses on the nonlinear static analysis of two sets of masonry panels. The walls under study were already experimentally out-of-plane tested at the University of McMaster and Plymouth by Gazzola and Drysdale (1986) and Chong et al. (1994), respectively. Also, it is highlighted that a refined mesh was defined for both case studies. The size of the interfaces (H), i.e. the side length of each quadrilateral panel, is only 100 mm.

In the first step, the holonomic homogenization model allows obtaining the macroscopic masonry material properties accounting for the strain softening regime. In the second step, this information should serve as input for the analysis at a structural level. Thus, the novel discrete element model implemented in the finite element package ABAQUS must be able to receive such data. The concrete damage plasticity model is selected for this purpose, as it allows to fully represent the inelastic behavior of masonry, by defining stress-strain curves for axial and torque trusses of the system. For further details concerning the model and its implementation, see Wahalathantri et al. (2011).

Simplified softening curves are considered for each truss, see for instance Fig. 5. To avoid convergence and run time problems, a small plateau near the peak of the curves is adopted in order to avoid abrupt stiffness losses. For the simulations, the post-failure stress-strain behavior must be introduced in the material information parameters. Specifically, ABAQUS requires the introduction of the cracking strain $\tilde{\varepsilon}_t^{ck}$, which can be obtained for each point of the homogenized curve by Eq.(12):

$$\tilde{\varepsilon}_t^{\,ck} = \varepsilon_t - \varepsilon_0^{el} \quad (12)$$

where ε_o^{el} is the elastic strain corresponding to the undamaged material and ε_t is the total strain of the holonomic curve. Damage parameters d_t should also be introduced, which link the undamaged elastic modulus with that of the damaged material in the unloading phase, as $E_d = E(1 - d_t)$, see also Fig. 5.

Macro-scale validation: out-of-plane loaded masonry panels

The macro-scale validation of the homogenization model is achieved by analyzing masonry panels subjected to out-of-plane loads. The aim is to conclude about the ability of the model to reproduce the nonlinear out-of-plane response of masonry. Available experimental data of windowed and full panels in two-way bending are used. The panels result from the studies of Gazzola and Drysdale (1986) at the University of McMaster and Chong et al. (1994) at the University of Plymouth.

The first set of panels that are being studied refers to three running bond masonry panels tested at the University of McMaster (Gazzola and Drysdale 1986). The panels are designated as WII, WF and WPI. The geometry of the panels is similar, being the boundary conditions the main difference, see Fig. 6. Such analyses allow to conclude about the ability of the model to describe the response in terms of pressure vs. out-of-plane displacements, and if the homogenized model is able to reproduce a pre-compression state (due to the analysis in WPI panel).

Information concerning the assumed mechanical properties is reported in Table 1. The out-of-plane behavior of a masonry wall is essentially ruled by the flexural strengths along vertical and horizontal directions, which are available for both studied panels. The properties identification is achieved by fitting the flexural strengths values with the ones reported by Lourenço (1997). The same values for the horizontal flexural strength, f_{tx} = 0.81 (N/mm^2), and for the vertical flexural strength, f_{ty}=0.40 (N/mm^2), are adopted. The bricks dimensions are 390×190×150 mm^3 and the thickness of the joints is 10 mm. The same strategy is conducted for the Plymouth panels. Assuming bricks elastic and that the non-linearity is restricted to the tensile regime, only mortar tensile strength and cohesion can be tuned, with a fixed softening with pre-assigned fracture energy. It is believed that the model is able to reproduce and predict well the response of masonry in the cases where sufficient experimental information on its constituents is available.

The refined mesh with 100 mm of size has 1196 discrete elements for each panel (each discrete element has 4 quadrilateral rigid plates). Whilst only collapse loads are reported in Gazzola and Drysdale (1986), the results discussion addresses also the obtained capacity curves. For each studied panel, Fig. 7 illustrates a comparison on global force-displacement curves between the present model and: (i) the experimental collapse load (McMaster university data), (ii) an anisotropic macro-model by Lourenço (2000) and (iii) an upper and lower bond limit analysis by Milani et al. (2006).

For all the panels and regarding the collapse load, the present model allows to reach an acceptable maximum error of 11% on peak experimental loads. Moreover, the pushover curves present a similar shape when compared with those provided by the macro-model proposed by Lourenço (2000). As aforementioned, the conducted analyses include a pre-compression state only for the panel WPI. The homogenized model was prepared also to compute the final stress-strain curves bearing a defined pre-compression state, assuming that it is maintained constant during the out-of-plane loading.

The second set of out-of-plane experimental data is constituted by the panels tested at the University of Plymouth by Chong et al. (1994). Five panels in running bond masonry texture using solid clay bricks were tested and designated by SB (Chong et al. 1994; Southcombe et al. 1995). The panels SB01 and SB05 have the same geometry, thus only four panels (SB01-SB04) are considered and represented in Fig. 8. The boundary conditions are the same for the four panels, i.e. laterally simply supported and fixed at the base. The experimental investigation aimed at a better insight on the role played by the openings size and shape.

The panels were loaded by air-bags until failure, whereas both the pressure and displacement at the middle span of the free edge were monitored. Thus, the comparison is here done in terms of pressure load and displacement in each masonry panel.

At a meso-scale, the mechanical properties adopted for the RVE characterization were already presented in Table 1. Bearing that according to the experimental data (Chong et al. 1994; Southcombe et al. 1995), the flexural uniaxial strengths f_{tx} and f_{ty} are 2.28 and 0.97 N/mm^2, respectively, the mechanical properties adopted were tuned in order to fit the latter values. The bricks dimensions are 215×65×102.5 mm^3 and the thickness of the joints is 10 mm.

The refined mesh with 100 mm of size has 1122 discrete elements for panel SB01/05, 892 elements for panel SB02, 987 elements for panel SB03 and 960 elements for panel SB04. It is important to stress that the mesh at the macro-scale is independent from the mesh adopted in the RVE at a meso-scale and from the masonry texture, i.e. units' geometry. Each nonlinear analysis, with the present refined mesh, took around 9 minutes in a computer with an Intel Core i7-4710MQ 2.50 GHz processor. This running time accounts for the pre-homogenization and calibration steps required before the analysis and could be minimized, if (1) a coarser mesh is adopted or (2) by analyzing a half part of the wall due to symmetry conditions. It is also important to understand that softening is being represented and the associated convergence problems cannot be avoided.

Fig. 9 shows the comparison between the numerical and experimental results (Chong et al. 1994), concerning pressure load and displacement at the middle node of the free edge. In addition to the present model, other results are represented, namely an anisotropic macro-model (Lourenço 2000), an elastic perfectly-plastic homogenized model designated as EPP-model (Milani and Tralli 2011), a simplified deteriorating model based on homogenized limit analysis designated as SD model (Milani and Tralli 2011) and finally a simplified quadratic programming elastic-plastic model by Milani and Tralli (2011), in which deterioration of interfaces (ultimate bending moment) is considered. For the sake of conciseness, the reader is referred to Lourenço (2000) and Milani and Tralli (2011), in order to analyze with further detail each of the aforementioned models.

In general, the comparison allows concluding that the obtained results are good, both in terms of collapse load and displacements prediction, see Fig. 9. For the panel SB01/05 the failure pattern indicates that cracking occurs as expected due to flexural failure at the fixed base of the wall, see Fig. 10. The cracking formation near the lateral supports, i.e. diagonal cracks, is also clear. For further comparison with the experimental failure modes, see Lourenço (1997). The peak load results are similar to the ones obtained experimentally, even if the softening range starts slightly before than the other reference curves.

For the second panel, designated as SB-02, the initial stiffness is marginally overestimated. This panel is the one with the largest opening in height. Nevertheless, reasonable agreement is found regarding the obtained peak load with a relative error of around 20% with the experimental curve. The damage patterns show cracking due to horizontal bending in the fixed base, vertical bending above the opening and the formation of diagonal cracks surrounding the corners and lateral supports.

To what concerns panel SB03, both peak load and curve shape are quite similar to the results by Lourenço (1997). The post-peak behavior is again characterized by the formation of the vertical crack above the opening. Also, as expected, the formation of diagonal cracks is evident at the opening sides and with the direction of the lateral supports.

At last, the present model leads to a capacity curve with a reasonable agreement for the panel SB04, in which the peak load has a relative error of around 10% with the macro-model by Lourenço (1997). Similarly, a vertical crack above the opening is developed. Failure due to torsional movements is also visible around the lateral supports, as well as failure due to flexion at the base fixed support. The model is not able to directly follow diagonal yield lines (zig-zag instead). Even so, the used quadrilateral mesh is refined enough to minimize the mesh dependence and the differences concerning the experimental results are not significant.

The results show the capacity of the model to obtain good representations of the nonlinear behavior in panels with complex geometries, using refined meshes. The analyses of the Plymouth panels are repeated with less refined meshes, see Fig. 11. The goal is to evaluate the mesh dependence both in terms of results accuracy and running time duration. For the first panel (SB-01/05) three medium-high refinement meshes (in respect with the brick size) with edge size equal to 100, 150 and 200 mm, and two very coarse meshes, with edge size equal to 500 and 1000 mm, are compared. Fig. 11a demonstrates that the mesh dependency is low as the obtained difference on the pressure-displacement curve among the meshes is less than 15%, for such large variation of mesh sizes, which is acceptable from an engineering standpoint. In addition, it is worth noting that the required computational time is impressively reduced for the coarse meshes (less than one minute), but still reasonable for a strong mesh refinement, Fig. 11a (exponential reduction with the increase of mesh size). The deformed shapes of panel SB-01/05 for the four refinement levels studied are also presented in Fig. 11b.

On the other hand, only two refined meshes (150x150 mm^2 and 200x200 mm^2) were considered for the SB-02-04 panels to avoid geometrical misrepresentations, due to the existence of openings. Regarding the running time duration, the coarser mesh (200x200 mm^2) allows to obtain analyses times within 3 minutes only. For the peak load, the differences between the studied meshes are lower than 5%, being therefore not relevant for engineering applications. Some difference may be noted in the post-peak behavior, but it is well known that rigid elements, where nonlinearity is concentrated on interfaces, intrinsically suffer from limited mesh dependence on softening.

Conclusions

A two-step procedure was presented to study the nonlinear static behavior of masonry panels subjected to out-of-plane loading, and allowing the use of any standard advanced nonlinear finite element code. The first step concerns the homogenization model based on an elastoplastic approach. This is performed at a meso-scale through a FE discretization of the unit cell, the so-called representative volume element (RVE) and allows obtaining the curvature-bending moment diagrams for each direction, i.e. masonry orthotropy. For each layer, a plane-stress boundary problem was solved in which the nonlinearity is concentrated only on joint interfaces, accounting for both tensile and compressive strength and strain softening.

Being a new methodology, at a structural scale, the simulations were done within a novel discrete element model implemented in the Finite Element software package Abaqus (2006). The latter is composed by quadrilateral rigid plates connected by a system of rigid beams, axial and torque trusses. This system represents the behavior of the homogenized interfaces obtained previously. The obtained homogenized curves were calibrated and then scaled in order to be readable by the software.

The validation of the model was performed through nonlinear static analyses on masonry panels. The obtained peak loads have a good agreement with the experimental values with an error less than 20% for the peak load. Also, the shape of the capacity curves was compared with an anisotropic model. Good agreement was obtained between the capacity curves and damage patterns between the complex anisotropic model and the new discrete model, whereas a maximum peak load error of about 10% may be observed for the panel SB-02. In addition, a mesh dependency test was conducted to deepen the knowledge on refinement issues. One may note the importance of addressing the two following recommendations to practitioners interested in a fast and reliable analysis of masonry panels out-of-plane loaded: (i) the proposed homogenization-discrete element model does not show critical mesh dependence issues. Very coarse meshes proved to predict well the initial stiffness, ultimate load carrying capacity and ultimate ductility. The advantage of the utilization of coarse meshes is certainly the considerable reduced computation effort needed, see Fig. 11a. The only constraint is obviously in the correct definition of the possible location of yield lines compatible with the real ultimate behavior of the walls. On the other hand, (ii) as far as the previous precautions on the mesh generation are kept, the only limitation in the utilization of few rigid elements is the impossibility to obtain a detailed description of the actual crack patterns, to be compared with either experimental ones or those obtained from expensive micro-modelling strategies. When such output is needed, the user is recommended to refine the discretization.

At last, it is important to note the advantage of the procedure and its efficiency in respect with a detailed heterogeneous micro-modelling strategy (i.e. a separate discretization of bricks and mortar). The use of rigid plates minimizes the complexity regarding inelastic phenomena problems. Using standard commercial FE packages, the effectiveness and robustness of the software to solve problems accounting for the post-elastic behavior with softening can be used. This also allows the possibility to extend the use of the proposed model at professional level to fields such as earthquake or blast engineering. Regarding the former, the use of truss beam elements that reproduces the homogenized behavior of interfaces within a Concrete Damage Plasticity model at a macro-scale allows, in principle, to conduct numerical analyses in the non-linear dynamic range. In addition, the utilization of a robust commercial code like ABAQUS allows running analyses in the non-linear dynamic range without any special difficulty, because the ex-novo implementation of global solvers is not needed and proper hysteresis models are available. On the other hand, in what concerns the latter, the application of the model in the field of blast and impact engineering deserves a separate discussion because, in such case, mechanical properties of the constituent materials are rate-dependent. A practical way of proceeding would be to define the material properties using dynamic increase factors.

Acknowledgements

This work was supported by FCT (Portuguese Foundation for Science and Technology), within ISISE, scholarship SFRH/BD/95086/2013. This work was also partly financed by FEDER funds through the Competitivity Factors Operational Programme - COMPETE and by national funds through FCT – Foundation for Science and Technology within the scope of the project POCI-01-0145-FEDER-007633.

References

Abaqus. (2006). "Dassault Systèms Simulia Corporation." RI: Dassault Systèmes Simulia Corporation, Providence.

Akhaveissy, A. H., and Milani, G. (2013). "A numerical model for the analysis of masonry walls in-plane loaded and strengthened with steel bars." *International Journal of Mechanical Sciences*, Elsevier, 72, 13–27.

Anthoine, A. (1995). "Derivation of the in-plane elastic characteristics of masonry through homogenization theory." *International Journal of Solids and Structures*, 32(2), 137–163.

de Buhan, P., and de Felice, G. (1997). "A homogenization approach to the ultimate strength of brick masonry." *Journal of the Mechanics and Physics of Solids*, 45(7), 1085–1104.

Casolo, S., and Milani, G. (2010). "A simplified homogenization-discrete element model for the non-linear static analysis of masonry walls out-of-plane loaded." *Engineering Structures*, 32(8), 2352–2366.

Casolo, S., and Milani, G. (2013). "Simplified out-of-plane modelling of three-leaf masonry walls accounting for the material texture." *Construction and Building Materials*, 40, 330–351.

Cecchi, A., and Milani, G. (2008). "A kinematic FE limit analysis model for thick English bond masonry walls." *International Journal of Solids and Structures*, 45(5), 1302–1331.

Cecchi, A., Milani, G., and Tralli, A. (2007). "A Reissner–Mindlin limit analysis model for out-of-plane loaded running bond masonry walls." *International Journal of Solids and Structures*, 44(5), 1438–1460.

Chong, V., Southcombe, C., and May, I. (1994). "The behavior of laterally loaded masonry panels with openings." *Proceedings of 3rd international masonry conference. London, UK: Proceedings of the British Masonry Society*, 178–82.

Dhanasekar, M., Kleeman, P., and Page, A. (1985). "The failure of brick masonry under biaxial stresses." *ICE Proceedings*, Thomas Telford, 79(2), 295–313.

Gazzola, E. A., and Drysdale, R. G. (1986). "A Component Failure Criterion for Blockwork in Flexure." *Advances in Analysis of Structural Masonry*, ASCE, 134–154.

Gilbert, M., Casapulla, C., and Ahmed, H. M. (2006). "Limit analysis of masonry block structures with non-associative frictional joints using linear programming." *Computers & Structures*, 84(13–14), 873–887.

Kawai, T. (1977). "New Discrete Structural Models and Generalization of the Method of Limit Analysis." *Finite Elements in Nonlinear Mechanics, P.G. Bergan et al. eds*, Tapir Publishers, 885–906.

Lourenço, P. B. (1997). "An anisotropic macro-model for masonry plates and shells: implementation and validation." *TNO Building and Construction Research - Computational Mechanics*, (report no. 03.21.1.31.07), 34–91.

Lourenço, P. B. (2000). "Anisotropic Softening Model for Masonry Plates and Shells." *Journal of Structural Engineering*, American Society of Civil Engineers, 126(9), 1008–1016.

Lourenço, P. B., Rots, J. G., and Blaauwendraad, J. (1998). "Continuum Model for Masonry: Parameter Estimation and Validation." *Journal of Structural Engineering*, American Society of Civil Engineers, 124(6), 642–652.

Luciano, R., and Sacco, E. (1997). "Homogenization technique and damage model for old masonry material." *International Journal of Solids and Structures*, 34(24), 3191–3208.

Macorini, L., and Izzuddin, B. A. (2011). “A non-linear interface element for 3D mesoscale analysis of brick-masonry structures.” *International Journal for Numerical Methods in Engineering*, 85(12), 1584–1608.

Macorini, L., and Izzuddin, B. A. (2013). “Nonlinear analysis of masonry structures using mesoscale partitioned modelling.” *Advances in Engineering Software*, 60–61, 58–69.

Massart, T. J., Peerlings, R. H. J., and Geers, M. G. D. (2007). “An enhanced multi-scale approach for masonry wall computations with localization of damage.” *International Journal for Numerical Methods in Engineering*, John Wiley & Sons, Ltd., 69(5), 1022–1059.

Memon, B.-A., and Su, X. (2004). “Arc-length technique for nonlinear finite element analysis.” *Journal of Zhejiang University. Science*, 5(5), 618–28.

Mercatoris, B. C. N., and Massart, T. J. (2011). “A coupled two-scale computational scheme for the failure of periodic quasi-brittle thin planar shells and its application to masonry.” *International Journal for Numerical Methods in Engineering*, John Wiley & Sons, Ltd., 85(9), 1177–1206.

Milani, G. (2011). “Simple homogenization model for the non-linear analysis of in-plane loaded masonry walls.” *Computers & Structures*, 89(17), 1586–1601.

Milani, G., and Lourenço, P. B. (2010). “A simplified homogenized limit analysis model for randomly assembled blocks out-of-plane loaded.” *Computers & Structures*, 88(11–12), 690–717.

Milani, G., Lourenço, P., and Tralli, A. (2006). “Homogenization Approach for the Limit Analysis of Out-of-Plane Loaded Masonry Walls.” *Journal of Structural Engineering*, American Society of Civil Engineers, 132(10), 1650–1663.

Milani, G., Lourenço, P., and Tralli, A. (2007). “3D homogenized limit analysis of masonry buildings under horizontal loads." *Engineering Structures*, 29(11), 3134–3148.

Milani, G., and Tralli, A. (2011). "Simple SQP approach for out-of-plane loaded homogenized brickwork panels, accounting for softening." *Computers & Structures*, 89(1–2), 201–215.

Milani, G., and Venturini, G. (2011). "Automatic fragility curve evaluation of masonry churches accounting for partial collapses by means of 3D FE homogenized limit analysis." *Computers & Structures*, 89(17–18), 1628–1648.

Mistler, M., Anthoine, A., and Butenweg, C. (2007). "In-plane and out-of-plane homogenisation of masonry." *Computers & Structures*, 85(17), 1321–1330.

Pegon, P., and Anthoine, A. (1997). "Numerical strategies for solving continuum damage problems with softening: Application to the homogenization of Masonry." *Computers & Structures*, 64(1–4), 623–642.

Pelà, L., Cervera, M., and Roca, P. (2013). "An orthotropic damage model for the analysis of masonry structures." *Construction and Building Materials*, 41, 957–967.

Southcombe, C., May, I., and Ching, V. (1995). "The behavior of brickwork panels with openings under lateral load." *Proceedings of the 4th international masonry conference, vol. 1*, British Masonry Society, London, 105–10.

Wahalathantri, B. L., Thambiratnam, D., Chan, T., and Fawzia, S. (2011). "A material model for flexural crack simulation in reinforced concrete elements using ABAQUS." *Proceedings of the First International Conference on Engineering, Designing and Developing the Built Environment for Sustainable Wellbeing*, Queensland University of Technology.

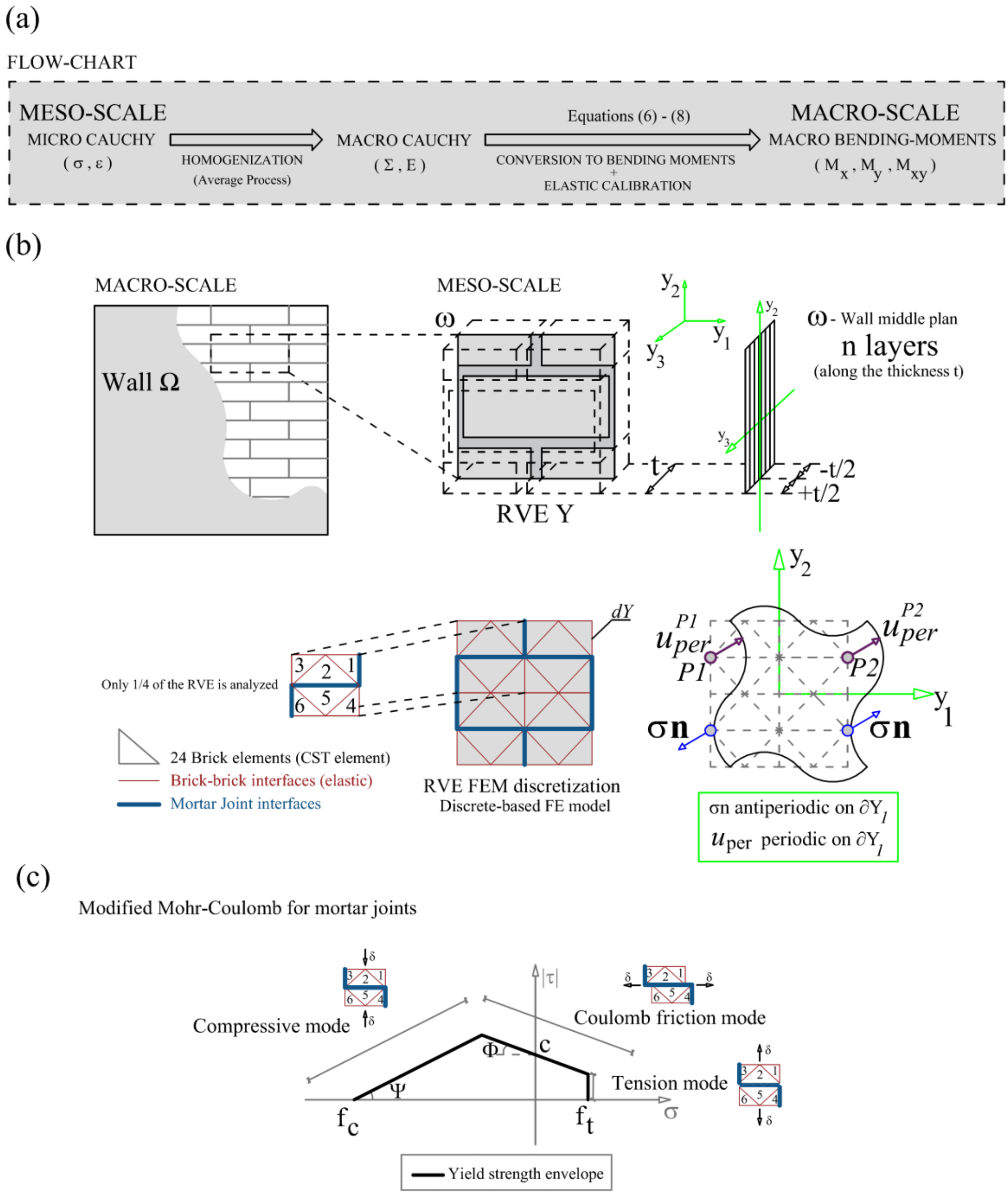

Fig. 1. (a) Flow-chart of the present two-step procedure; (b) Micro-mechanical model adopted for the present homogenized model; and (c) strength domain for joints reduced to interfaces.

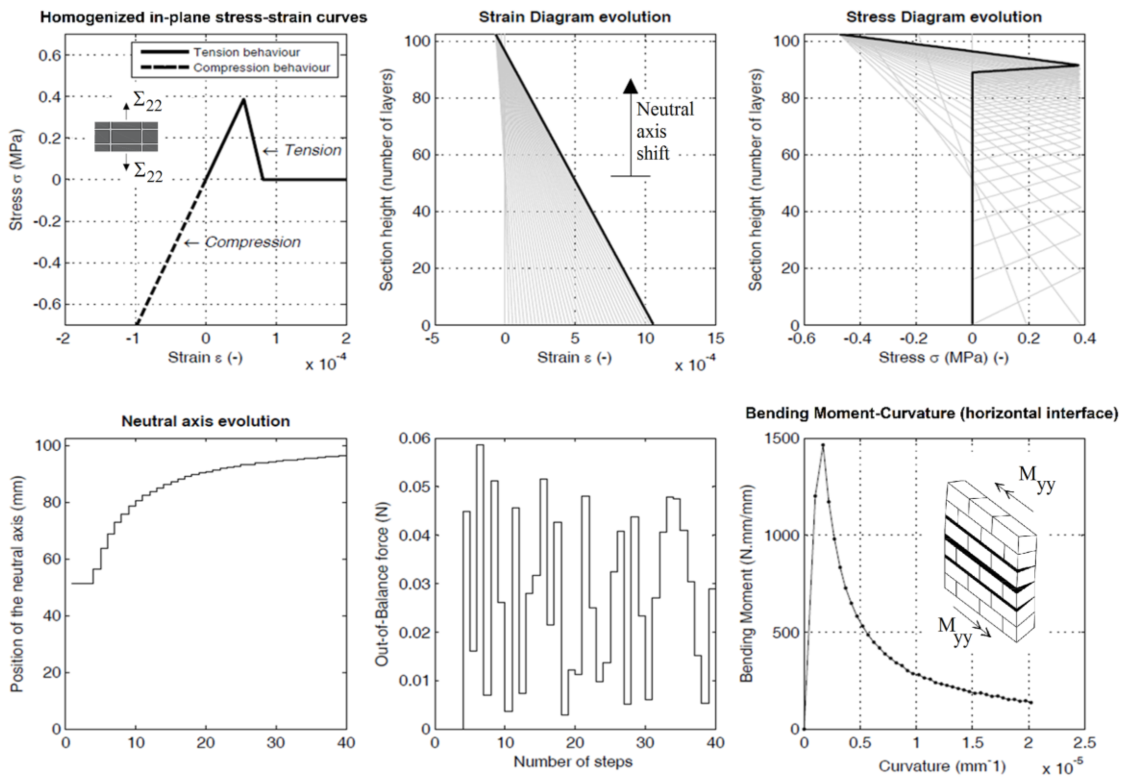

Fig. 2. Adopted procedure to derive out-of-plane homogenized bending moment-curvature curves (e.g. vertical bending).

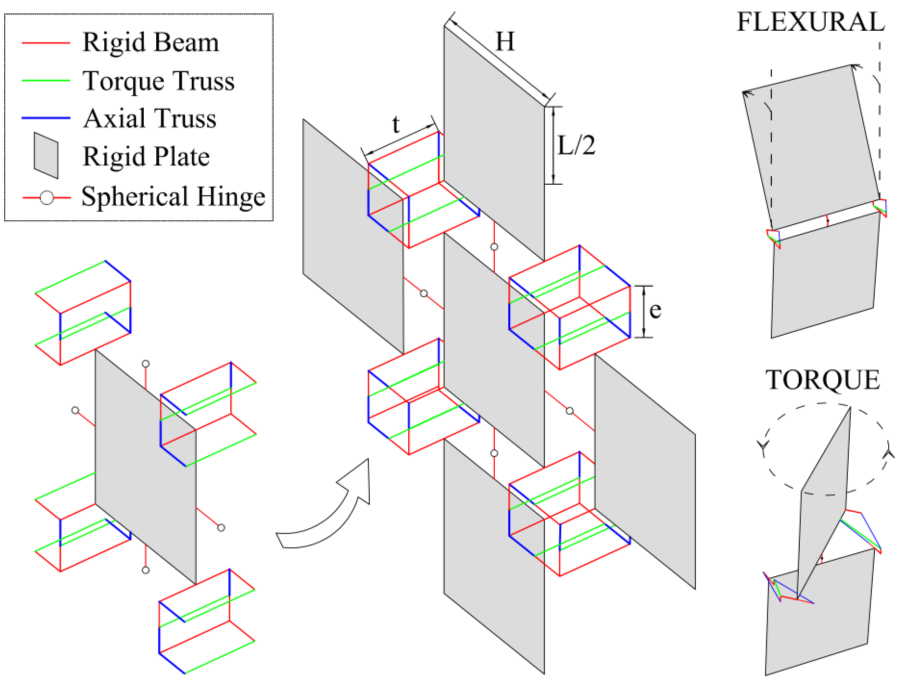

Fig. 3. Description of the novel discrete element system proposed.

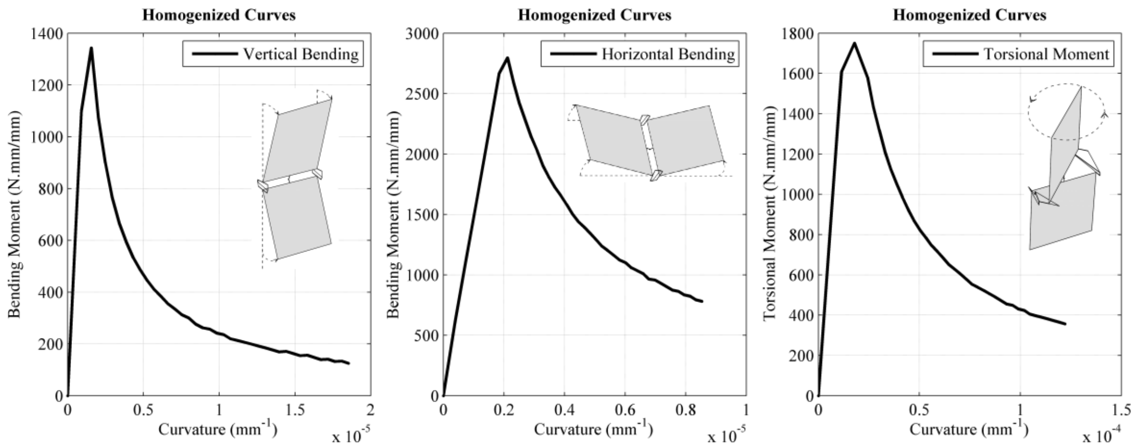

Fig. 4. Calibrated bending moment and torsional moment homogenized curves for the study of the panels tested by Chong et al. (1994).

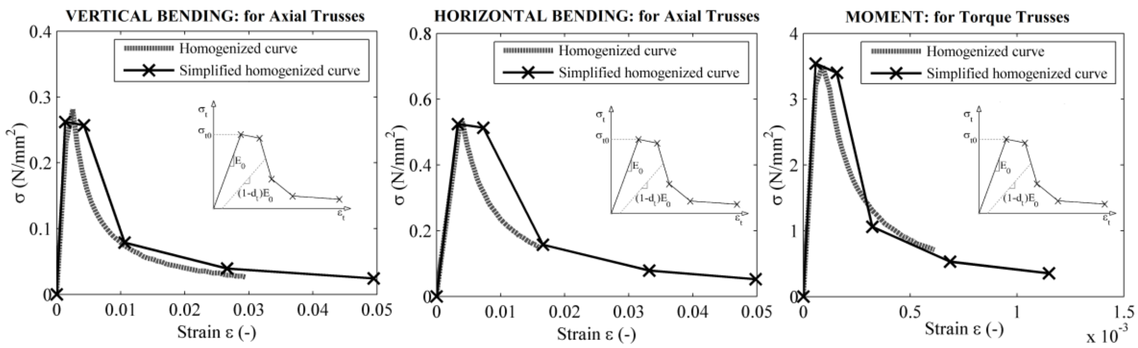

Fig. 5. The calibrated stress-strain curves obtained for the panels tested experimentally by Chong et al. (1994) at the University of Plymouth; input curves for each truss beam of the discrete system.

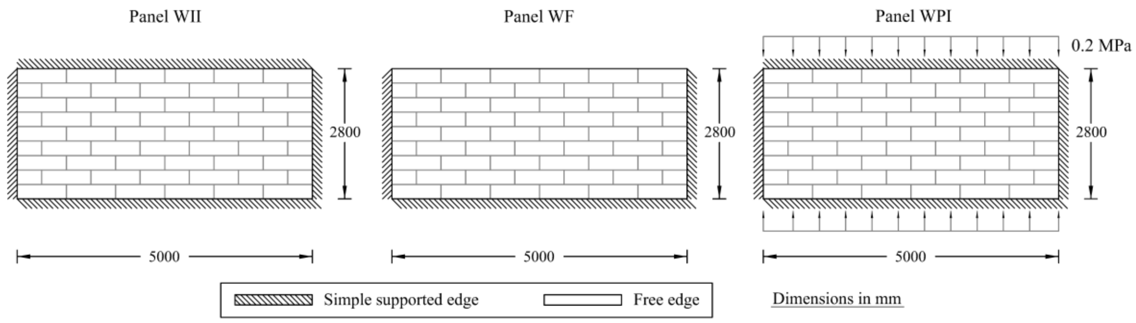

Fig. 6. Masonry panels out-of-plane loaded at University of McMaster (Gazzola and Drysdale 1986); description of the geometry and boundary conditions.

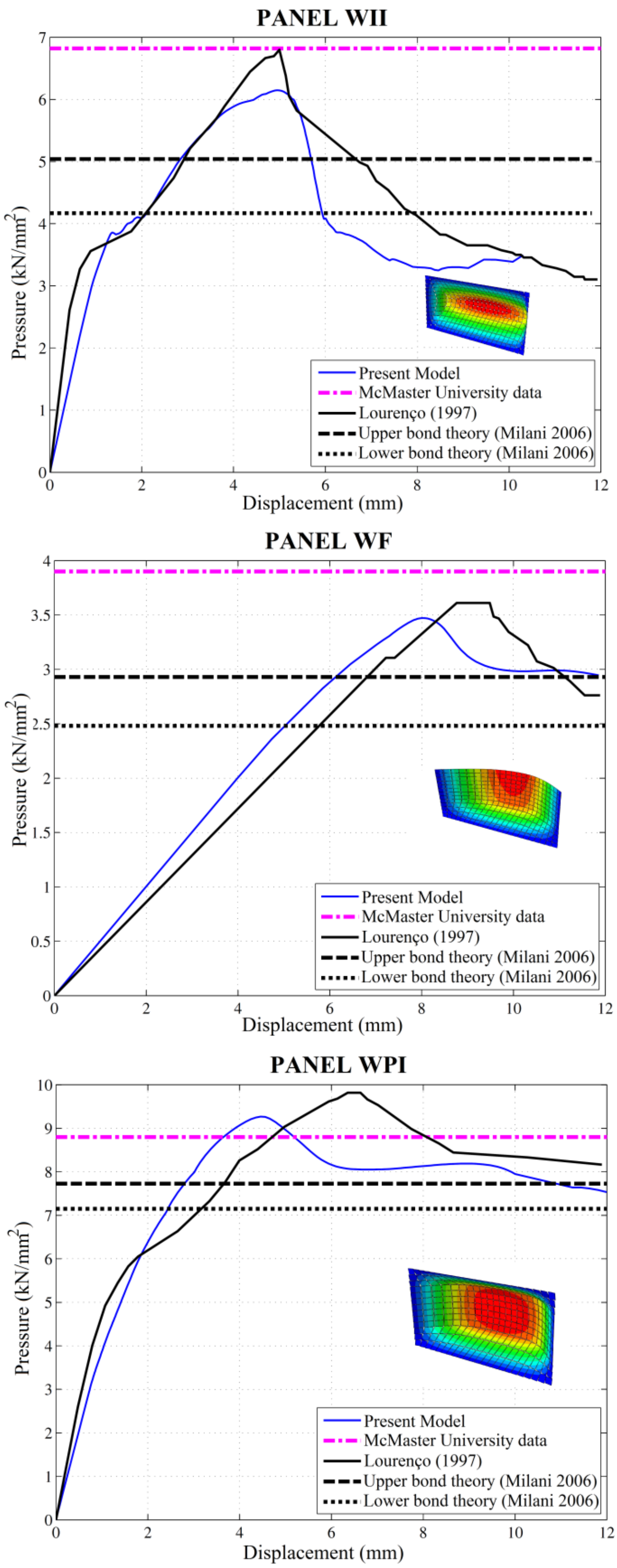

Fig. 7. Numerical and experimental curves of the panels experimentally tested by Gazzola and Drysdale (1986): pressure load vs displacement.

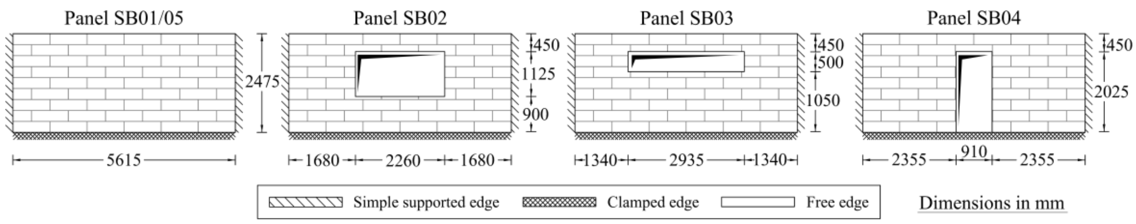

Fig. 8. Masonry panels out-of-plane loaded at University of Plymouth (Chong et al. 1994); description of the geometry and boundary conditions.

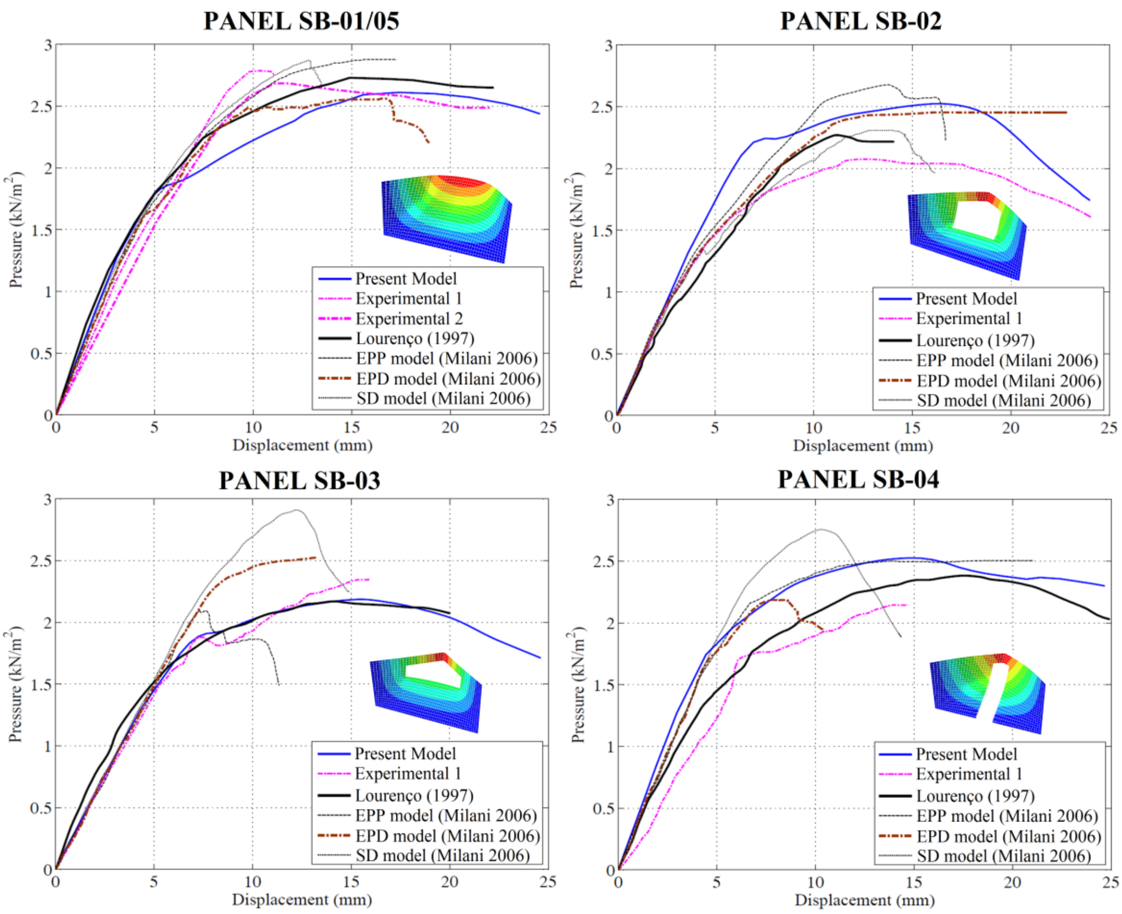

Fig. 9. Numerical and experimental curves of the panels experimentally tested by Chong et al. (1994): pressure load vs displacement and deformed shapes at ultimate load level.

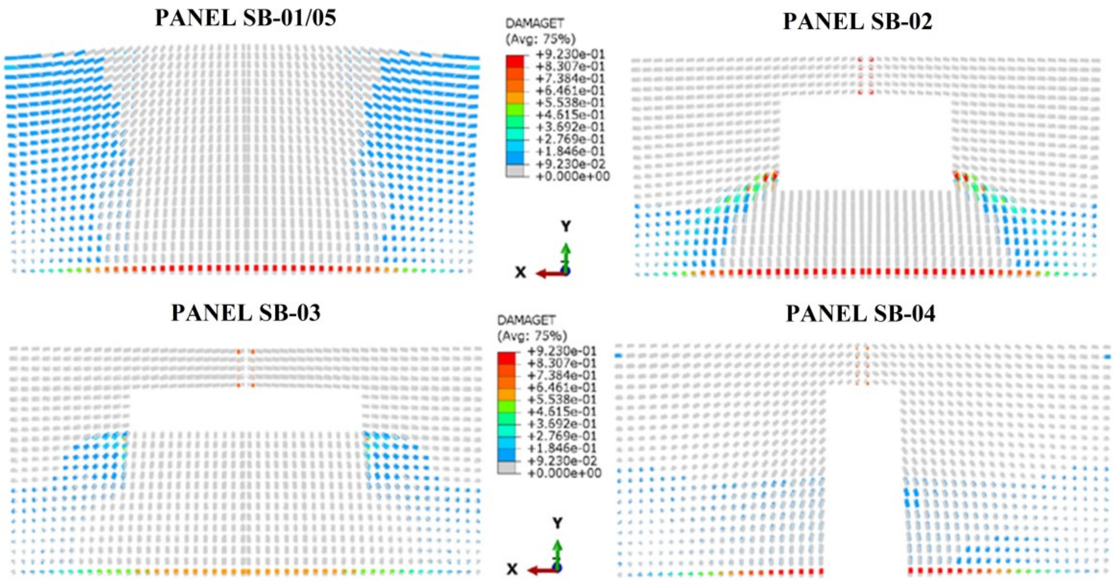

Fig. 10. Damage patterns obtained from the numerical analyses (ultimate load).

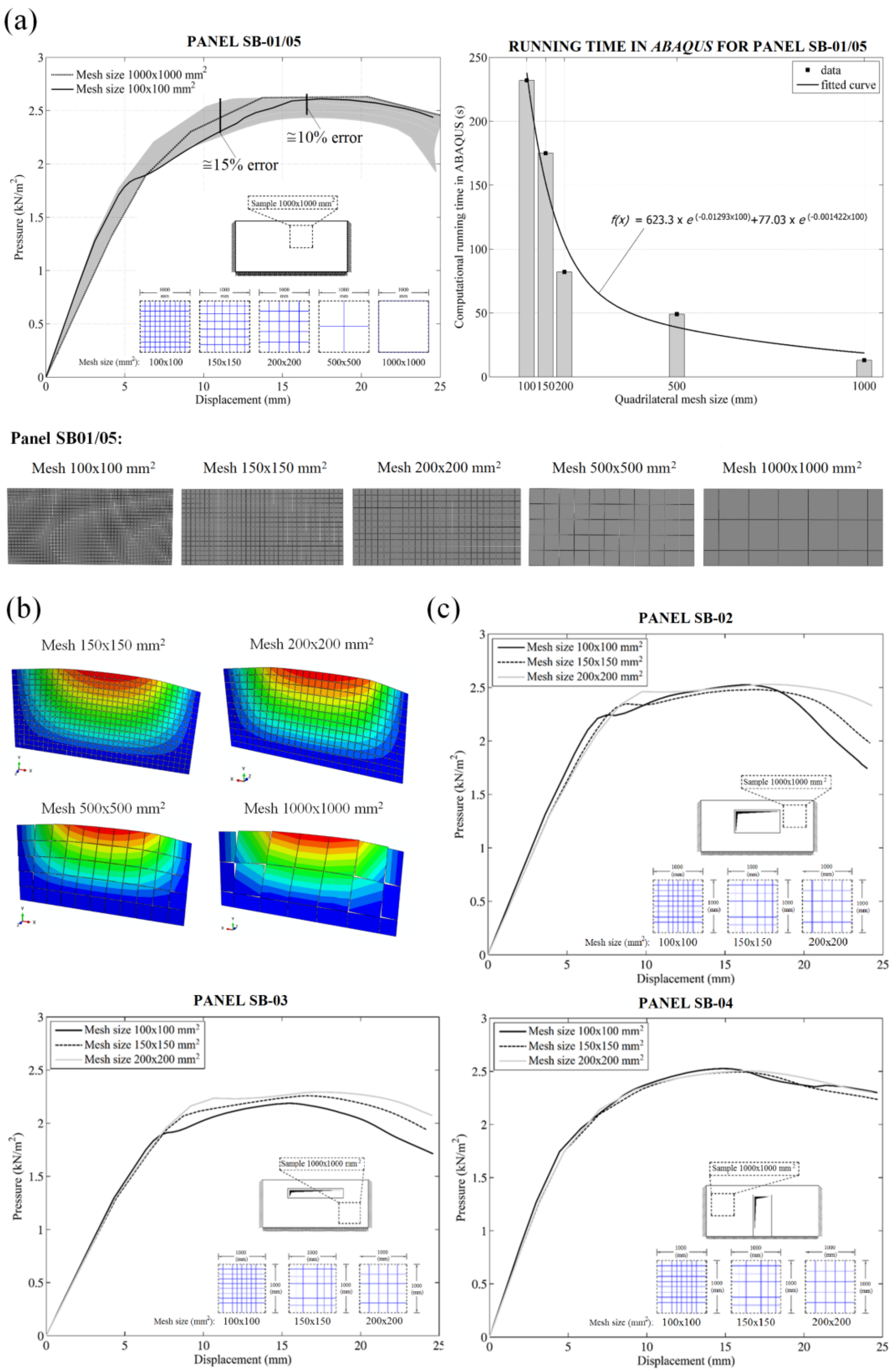

Fig. 11. (a) Mesh dependence for the SB-01/05 panel; (b) deformed shapes for the less refined meshes for Panel SB-01/05; (c) mesh dependence study for the SB-02, SB-03 and SB-04 panels.

Table 1. Mechanical properties adopted for the homogenization step for both McMaster and Plymouth University panels.

Parameter	Panels	
	McMaster	Plymouth
Young's Modulus of the mortar (MPa)	4000	3500
Young's Modulus of the brick (MPa)	15000	10000
Poisson coefficient (-)	0.20	0.20
Shear Modulus (MPa)	2000	1500
Cohesion, c (MPa)	1.6 x f_t	1.2 x f_t
Tensile strength f_t (MPa)	0.35	0.52
Compressive strength f_c (MPa)	20.0	2.0
Friction angle (ϕ) (degrees)	30.0	30.0
Linearized compressive cap angle (ψ) (degrees)	45.0	50.0
Mode I fracture energy, G_f^I (N/mm)	0.018	0.010
Mode II fracture energy, G_f^{II} (N/mm)	0.022	0.012
Elastic Parameters (for a mesh size: H = 100 mm; e=10 mm)		
K_n - axial truss (MPa)	236.74	157.83
K_n - torque truss (MPa)	191761	27874
Axial truss area (mm^2)	3750	2562.5
Torque truss area (mm^2)	500	500